Visual Psychophysics and Physiological Optics

Multichannel Functional Testing in Normal Subjects, Glaucoma Suspects, and Glaucoma Patients

Alfonso Antón,[1–3] *Pascual Capilla,*[4] *Antonio Morilla-Grasa,*[1] *María José Luque,*[4] *José María Artigas,*[4] *and Adelina Felipe*[4]

PURPOSE. To evaluate visual function with a novel multichannel functional test named the ATD Multichannel Functional Test.

METHODS. This multicenter study had a prospective and cross-sectional design. A total of 186 eyes were included: 42 with glaucoma, 14 glaucoma suspects due to optic nerve characteristics, 25 ocular hypertensives, and 105 normal eyes. All patients performed standard visual fields (Humphrey 24-2) and ATD with eight stimuli configurations: four achromatic (A), two red-green (T), and two blue-yellow (D). To derive main outcome measures, mean sensitivity, mean defect (MD), and pattern standard deviation (PSD) were calculated and compared among groups and types of stimuli with the Kruskal-Wallis test. The percentage of cases outside normal limits (ONL) was calculated.

RESULTS. MD and PSD were significantly different in glaucoma eyes than in normal subjects for all types of stimuli except D-0.5 cycles per degree (cpd)/12Hz. PSD was also lower for normals than for all pathologic groups with A-4cpd/2Hz, A-4cpd/12Hz, D-0.5cpd/2Hz, and T-0.5cpd/2Hz. The highest percentage of ONL cases was obtained with the two low-spatial-frequency chromatic stimuli, with D-0.5cpd/2Hz and T-0.5cpd/2Hz using PSD, which classified as ONL 81.6% and 86.7% of glaucoma eyes, 51.8% and 44.5% of hypertensives, and 72.2% and 41.2% of optic disc suspects, respectively.

CONCLUSIONS. ATD assessed different aspects of visual function, and the most sensitive tests to detect glaucomatous damage were the low-temporal-frequency chromatic tests. (*Invest Ophthalmol Vis Sci.* 2012;53:8386–8395) DOI:10.1167/iovs.12-9944

Glaucoma management is based on the assessment of structural and functional optic nerve damage in conjunction with intraocular pressure (IOP) control.[1] Standard

automated perimetry (SAP) has limited sensitivity for detecting early glaucomatous damage because detection of structural damage with existing clinical tools may precede SAP defects by several years, and up to 40% of retinal ganglion cells may be lost before SAP becomes abnormal.[2–4] Different functional tests have been developed to overcome the limitations of SAP, that is, lack of sensitivity, variability, learning curve, and lack of selectiveness for any particular ganglion cell type. Some tests have been developed to preferentially evaluate the koniocellular pathway, such as short-wavelength automated perimetry (SWAP)[5,6]; others, such as motion detection perimetry (MAP),[7,8] frequency-doubling technology (FDT),[9–12] and pulsar perimetry, were initially designed to favor the magnocellular pathway.[13–15] Still other tests, such as high-pass resolution perimetry (HPRP),[16,17] were developed to evaluate and facilitate detection by means of the parvocellular pathway. Whether these techniques do really isolate a single mechanism is doubtful, and it has been recently shown, for instance, that FDT does not preferentially evaluate the magnocellular pathway.[12] The relative efficacy of these techniques is also under discussion. Although there is evidence that SWAP,[8,18,19] FDT,[18,20] HPRP,[16] and MAP[8] detect functional deficits before they are identified by SAP, other studies have found similar glaucoma detection capabilities with SAP, SWAP,[21,22] FDT,[21,23] and HPRP.[24]

Despite the development of all these functional tests, SAP is still the clinical standard for most physicians.[1] In this scenario we have developed, and evaluated, a new psychophysical multichannel test named the ATD Multichannel Functional Test. "A," "T," and "D" in different color vision models stand for the three postreceptoral mechanisms—achromatic, red-green (because this is the color mechanism left to tritanopes, hence the "T") and blue-yellow (because this is the color mechanism left to deuteranopes, hence the "D"). Since this notation system is not usual in clinical research, in what follows we use "RG" and "BY" instead when referring to the chromatic mechanisms. The ATD test performs contrast sensitivity measurements with sinusoidally modulated patterns at any frequency in space and time and along any direction of the opponent modulation space or DKL space (named after Derrington, Krauskopf, and Lennie[25]). The rationale of the device is that a pattern modulated in the cardinal direction of a given postreceptoral mechanism (i.e., the directions in the color space isolating that mechanism), and having appropriate spatial and temporal characteristics, favors a particular physiological pathway.[26]

Comparison between visual pathways in terms of the magnitude of the functional damage has been usually made with tests that measure properties of a different nature for each pathway.[16,27] We believe that using the same psychophysical task for all three pathways could facilitate the assessment and comparison of the relative damage suffered by each. Several studies have attempted to evaluate the utility of assessing thresholds of the different mechanisms. In monkeys,

TABLE 1.   Groups: Criteria and Demographics

	Normal	Glaucoma	OHT-S	RNFL-S
IOP, mm Hg	≤21	Any	≥22	Any
Visual field	Normal	Glaucomatous	Normal	Normal
Optic nerve	Normal	Glaucomatous	Normal	Normal
OCT	Normal	Not considered	Normal	ONL
Number	105	42	25	14
Age				
Mean ± SD	55 ± 10	66 ± 10	60 ± 11	62 ± 10
Range	36 to 75	41 to 74	39 to 75	39 to 74
Men/Women				
Number	58/46	20/22	7/18	11/3
Percentage	56/44	48/52	28/72	78/22
SAP-MD, dB				
Mean ± SD	−0.4 ± 1.2	−6.8 ± 6.3	−0.3 ± 1.4	−1.9 ± 2.3
Range	−3.3 to 1.5	−23.1 to −2.2	−3.2 to 3.7	−7.8 to 1.7
SAP-PSD, dB				
Mean ± SD	1.7 ± 0.5	6.4 ± 3.6	1.7 ± 0.4	3.0 ± 1.3
Range	1.0 to 3.6	1.4 to 14.1	0.8 to 2.7	1.1 to 5.8

this has been evaluated by Harwerth et al.[28] for experimental glaucoma. King-Smith and colleagues[29,30] evaluated color contrast thresholds for different mechanisms in glaucoma and found that in certain cases it was the red-green opponent pathways that first revealed the deficits. In human subjects, Johnson et al.[31,32] found that red-green opponent process perimetry sometimes revealed the earliest deficits. ATD evaluates the three pathways with the same type of stimuli and may offer a customizable clinical tool for glaucoma management. The purpose of this study was to assess eight different ATD examination protocols in normal subjects, glaucoma suspects, and glaucoma patients.

METHODS

This was a cross-sectional study with prospective selection of 186 eyes from 186 subjects. One eye was randomly selected if both eyes met study criteria. Participants underwent a thorough ophthalmic examination, refraction, slit-lamp biomicroscopy, IOP measurement with Topcon CT-80 (normal subjects) (Topcon, Tokyo, Japan) or Goldmann tonometry (patients), Farnsworth-Munsell 100-Hue color test, standard achromatic perimetry (SAP) (Humphrey Field Analyzer II; Zeiss Meditec, Oberkochen, Germany) with the 24-2 SITA-Standard algorithm, ATD perimetry with eight different stimuli (see below), and optic nerve head assessment by a glaucoma specialist at the slit lamp. If pathologic signs were identified, stereophotographs were obtained for confirmation. Optic nerve head photography (TRC-50IX; Topcon) and optical coherence tomography (OCT Stratus; Zeiss Meditec) were also performed in suspects and patients. Exclusion criteria were spherical equivalent over +5 or under −5 diopters; visual acuity worse than 20/30; presence of ocular, neurological, or systemic diseases that could alter visual function; previous ocular surgery (except for uneventful phacoemulsification); and, for normals, any color deficiencies identified by the Farnsworth-Munsell 100-Hue color test. Only eyes classified as "average discrimination" by the color test were included. Eyes with mild cataract and no lens color changes were accepted. Reliable SAP fields, with fixation losses <20% and both false-positive and false-negative rates <30%, were required.

Subjects were assigned to one of four groups based on SAP results, optic disc appearance, optical coherence tomography (OCT), and IOP, following the specific classification criteria in Table 1.

Forty-two eyes had glaucoma (G); 14 eyes were glaucoma suspects with nerve fiber layer thinning (RNFL-S); 25 eyes were glaucoma suspects due to high IOP (ocular hypertensive subjects [OHT-S]); and 105 eyes were normal (N). SAP visual fields were defined as glaucomatous if they showed a cluster of three or more adjacent locations at 5% or less probability of normality, with one or more of those points at 1% or less probability on the pattern deviation map and confirmed on two or more fields. All glaucoma subjects included had an early to moderate degree of the disease (SAP mean defect of −2.2 to −23.1 dB). The optic disc was considered glaucomatous if any of the following features were identified: neuroretinal rim thinning, notch, disc hemorrhage, nerve fiber layer defect, asymmetry of vertical cup-to-disc ratio of 0.3 or more unexplainable by disc size asymmetry, or a cup-to-disc ratio of 0.8 or more unexplainable by a large disc size. Finally, OCT was considered abnormal when one or more quadrants were outside 95% normal limits for two consecutive images.

ATD Functional Test

Device. Stimuli were generated on a 17-inch LG Flatron F700P CRT monitor (LG Electronics, Inc., Youngdungpo-gu Seoul, Korea) configured to have a horizontal resolution of 1280 lines and a frame rate of 72 Hz, driven by a Bits++ video controller of 12 bits provided by Cambridge Research Systems (Rochester, UK). The system was colorimetrically characterized and gamma corrected using a ColorCAL colorimeter and the Cambridge Research Systems Toolbox for MATLAB.

Stimulus Description. Stimuli were spatiotemporal sinusoidal patterns, with smoothed borders, 5° × 5° in size and with a maximum duration of 1 second, modulated along the cardinal directions of the achromatic (A), red-green (RG), and blue-yellow (BY) mechanisms of the opponent modulation or DKL space (i.e., the directions isolating each mechanism).[25,33–35]

To describe the spatiotemporal characteristics of the stimulus, let us define a coordinate system (x', y', t') with origin of spatial positions at the center of the display, which serves as the fixation point for the observer, and origin of time at the beginning of the test presentation.
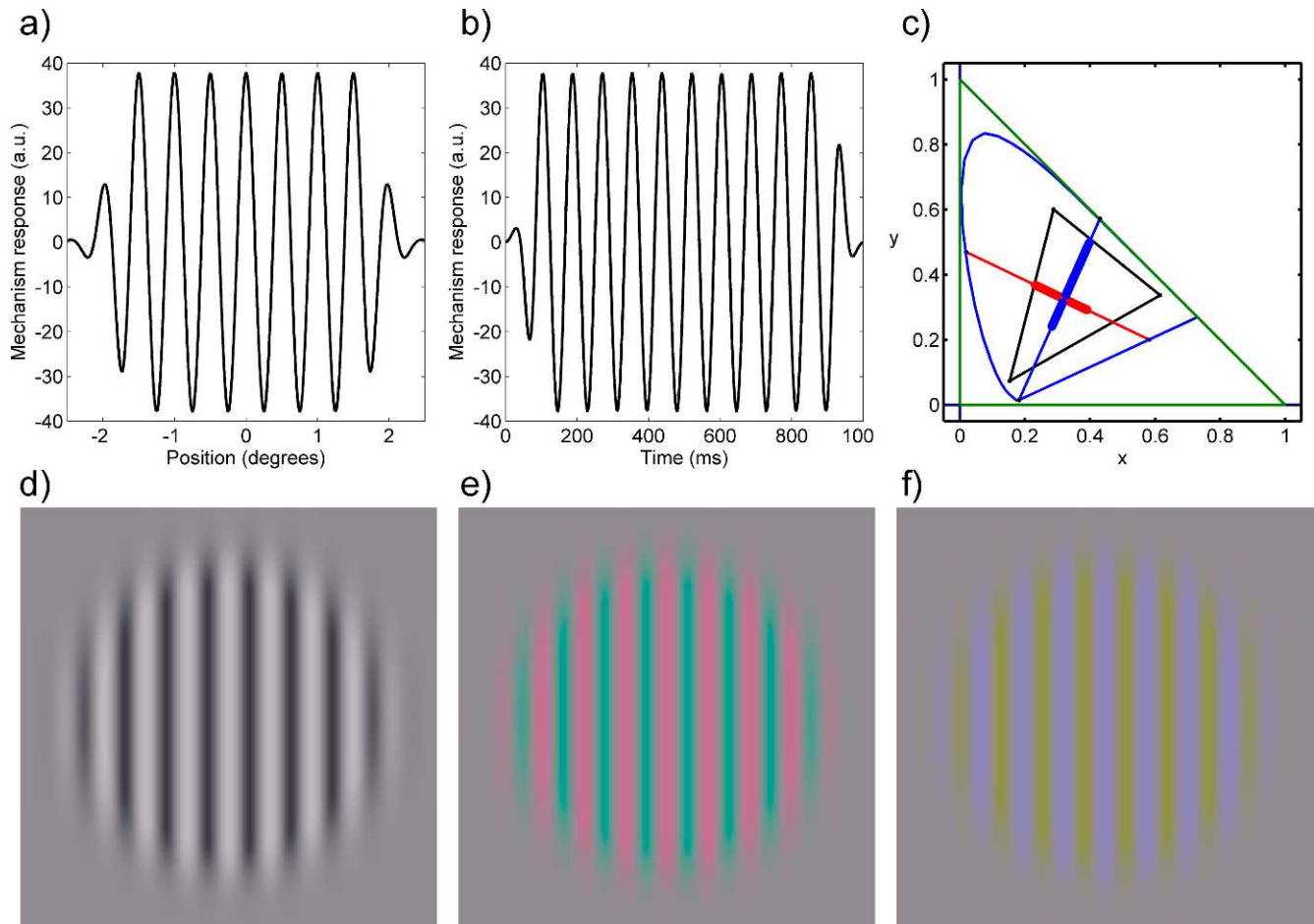
FIGURE 1. (a) Spatial profile of a stimulus as shown in the CRT. (b) Temporal profile. (c) Color palettes for the chromatic gratings. (d–f) Spatial appearance of the patterns favoring the achromatic, red-green, and blue-yellow mechanisms.

At each trial, a stimulus centered at a given location (x'_C, y'_C) is shown at the instant t'_0. At each position (x, y) relative to the center of the stimulus (with $x = x' - x'_C$ and $y = y' - y'_C$) and for each instant $t = t' - t'_0$ after stimulus onset, the spatiotemporal patterns are described by the following equation:

$$\begin{pmatrix} \Delta A(x,y,t) \\ \Delta RG(x,y,t) \\ \Delta BY(x,y,t) \end{pmatrix} = \begin{pmatrix} \Delta A_s \\ \Delta RG_s \\ \Delta BY_s \end{pmatrix} \cdot sen\left(2\pi f_x x + \frac{\pi}{2}\right) \cdot sen\, 2\pi f_t t \cdot g(r) \cdot b(t)$$

$$\cdot\, rect\left(\frac{x}{a}, \frac{y}{a}\right) \qquad (1)$$

The vector components, ΔA_s, ΔRG_s, and ΔBY_s, are the maximal response variations—or amplitudes—elicited by the pattern in the achromatic, red-green, and blue-yellow mechanisms, measured from the response values corresponding to the average stimulus, which is the achromatic stimulus of the display ($x_{CIE} = 0.2709$, $y_{CIE} = 0.2966$) with a luminance of 45 cd/m². Two of these vector components must be zero to isolate a given mechanism. The function $g(r)$, with $r^2 = x^2 + y^2$, is a spatial envelope with radial symmetry, defined as:

$$g(r) = \begin{cases} 1 & if \quad 0 \leq r \leq r_0 \\ \exp\left\{-\dfrac{(r - r_0)^2}{2\sigma^2}\right\} & if \quad r > r_0 \end{cases} \qquad (2)$$

where $r_0 = 1.5°$ and $\sigma = (1/3)°$. The function $b(t)$ is a temporal envelope, defined as:

$$b(t) = \begin{cases} \exp\left\{-\dfrac{(t - t_0)^2}{2\sigma_t^2}\right\} & if \quad 0 \leq t \leq t_0 \\ 1 & if \quad t_0 < t \leq T_s - t_0 \\ \exp\left\{-\dfrac{(t - T_s + t_0)^2}{2\sigma_t^2}\right\} & if \quad T_s - t_0 < t \leq T_s \end{cases} \qquad (3)$$
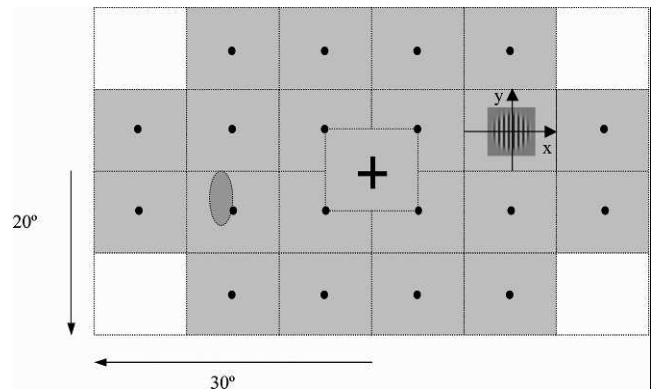

FIGURE 2. Spatial distribution of the 21 locations of the visual field where sensitivity was tested in the present study. The *cross* marks the fixation point, and the *oval patch* corresponds to the location of the blind spot for the left eye. An achromatic stimulus of the appropriate relative size is shown at a randomly chosen position.

where $T_s = 1000$ ms is the total presentation time, t_0 equals 100 ms, and $\sigma_t = t_0/3$. The role of these functions is to minimize spatial and temporal transients that may constitute a cue for detection by mechanisms different from the one we want to test. Finally, the rectangle function $rect\left(\frac{x}{a}, \frac{y}{a}\right)$, with $a = 5°$, limits the spatial extension of the stimuli. The limits and directions of the color palettes in the CIE chromaticity diagram, and examples of the spatial and the temporal profiles as well as a sample of stimuli in each of the cardinal directions, are shown in Figure 1.

In what follows, stimuli are labeled as mechanism (A, RG, or BY)-spatial frequency (0.5 or 4) in cycles per degree (cpd)/temporal frequency (2, 12, or 24) in Hertz (Hz). To evaluate the achromatic mechanism, two stimuli favoring the magnocellular pathway (A-0.5/12 and A-0.5/24) and two stimuli stimulating the parvocellular pathway (A-4/2 and A-4/12) were chosen. The red-green and blue-yellow chromatic mechanisms, putatively mediated by the parvo- and koniocellular pathways, respectively, were evaluated by two combinations of frequencies, 0.5/2 and 0.5/12. This procedure is similar to the one used by King-Smith and Carden for color contrast thresholds except that those investigators did not use sinusoidal gratings.[29]

Measurement Procedure. Measurements were carried out in a darkened room. During a session, contrast sensitivity was measured at the fovea and 20 locations forming a fovea-centered regular grid of 60° × 40° (see Fig. 2). After an adaptation period of 30 seconds, the fixation stimulus flickered to signal that the test was going to begin, and the first trial was presented. The subject was instructed to press the button if any variation from the background was detected at any point of the visual field. Subjects' responses caused the stimulus to disappear from the display but counted as detections only if they occurred 100 ms after stimulus onset and before stimulus offset. The maximum duration of the stimulus was 1 second. The time interval between trials was randomized by the program, from 200 to 500 ms, to minimize the likelihood that subjects would engage in rhythmic responses.

Thresholds were determined by an interleaved stepwise threshold algorithm. At each trial, the location of the stimulus changed at random. In the first trial at a given location, the stimulus had the maximum amplitude achievable by the CRT. If this stimulus was detected, amplitude was divided by 2 at the next trial in that location, and it continued decreasing in this way until the observer failed to detect the stimulus. The staircase was then reversed, and amplitude increased by a $\sqrt{2}$ factor for the next presentation and continued increasing in this way until the stimulus was again detected. This triggered a second reversal, and amplitude was divided by $\sqrt[4]{2}$, and so on. Thus, the amplitudes at two consecutive trials at the same location, ΔR_{k-1} and ΔR_k, relate to each other as follows:

$$\log_2(\Delta R_k) = \log_2(\Delta R_{k-1}) + \frac{(-1)^{n+1}}{2^n} \qquad (4)$$

where n is the number of reversals until trial k. The criteria for exiting the staircase procedure at a given location were totaling either four reversals or 20 presentations, whatever came first. The staircase was also interrupted at a given location if a series of five consecutive stimuli with maximum amplitude passed undetected. Once a staircase was finished, threshold at that location, ΔR_{thres}, was defined as the amplitude value of the last detected stimulus. If no stimulus was detected, threshold was defined as the maximum amplitude value achievable by the CRT in the corresponding cardinal direction. Contrast sensitivity, S, in decibels (dB) was computed as:

$$S = 10\log_{10}\frac{\Delta R_{\max}}{\Delta R_{thres}} \qquad (5)$$

where $\Delta R_{\max}$ is the maximum generable amplitude along the direction of the stimulus.

Reliability Assessment

Among the stimuli presentations, up to 16 false-positive trials and up to 10 false-negative trials were also randomly interleaved. Additionally, each session included up to eight fixation catch trials, presentations in the blind spot location previously estimated for the observer. These are 1.5° × 1.5° squares without Gaussian smoothing, and with the same chromatic and spatial modulation as the false-negative trials (achromatic with $f_x = 2$ cpd, without flicker), with maximum amplitude. Test results were rejected if the false-positive or the false-negative rate was over 33%, or if fixation losses had occurred over 20%.

Data Management

A normative database of contrast sensitivities was created with normal subjects arranged in 5-year bins for each stimulus type, each bin containing 10 subjects on average. Sensitivity data from each patient were compared to those for normal subjects in the same age range. Three global indices, the mean sensitivity (MS), the mean defect (MD), and the pattern standard deviation (PSD), were calculated for each visual field with Equations 6 through 8:

$$MS = \frac{1}{n}\sum_{i=1}^{n} S_{patient,i} \qquad (6)$$

where $S_{patient,i}$ is the sensitivity of the patient at location i in the visual field, in dB

$$MD = \frac{1}{n}\sum_{i=1}^{n} D_i \qquad (7)$$

$$PSD = \sqrt{\frac{1}{n-1}\sum_{i=1}^{n}(D_i - MD)^2} \qquad (8)$$

where the defect at location i, D_i, is computed as $D_i = S_{patient,i} - S_{standard,i}$; $S_{standard,i}$ is the mean sensitivity of the normal subjects of the same age group as the patient at location i; and n is the number of locations measured.

The following procedures were performed with each of these global indices, for each stimulus type:

1. Differences between population groups were assessed using multiple analysis of variance (ANOVA) with the Kruskal-Wallis test and the Tukey-Kramer post hoc test.
2. Cumulative distribution functions (CDFs) were obtained by means of the Kaplan-Meier algorithm[36] for each population group.
3. Cut points, defined as the value of the index verifying that 15% of the normal population yielded an equal or worse result, were computed by interpolating the CDF for normal subjects and were used to define normal limits.
4. The percentages of glaucoma, OHT-S, and RNFL-S classified as outside normal limits (ONL or hits) with these cut points were computed by interpolating their respective CDFs (see percentages in Table 3).
5. The differences among groups were analyzed with the χ^2 test, using the number of subjects classified as ONL in the sample (see the Hits/Total columns in Table 3).
6. Receiving operating characteristic (ROC) curves, plotting hit rate versus false-positive rates, were derived by counting, for each of the possible values of each global index, the number of normal and pathological subjects in our samples yielding a worse result (respectively, the false-positive rate, or 1–specificity, and the hit rate or sensitivity). The sensitivity values for 85% specificity and the point of best equilibrium between sensitivity and specificity (defined as the maximum mean value of sensitivity + specificity), obtained by interpolation of the

TABLE 2. ATD Global Indices by Group

Stimulus	Index	N	G	OHT-S	RNFL-S	Groups with Significant Differences	P Value
A-0.5/12	MS	12.7 ± 1.7	9.1 ± 2.8	13.4 ± 1.5	13.5 ± 1.0	* § ||	0.000
	MD	−0.5 ± 1.4	−3.6 ± 2.6	0.2 ± 1.2	0.3 ± 1.1	* ‡ ||	0.000
	PSD	1.7 ± 1.1	3.8 ± 1.5	2.3 ± 1.0	2.0 ± 0.7	* † § ||	0.000
A-0.5/24	MS	8.9 ± 1.8	6.2 ± 2.5	9.4 ± 2.0	9.2 ± 1.0	* § ||	0.000
	MD	−0.4 ± 1.5	−2.5 ± 2.4	0.3 ± 1.5	−0.2 ± 1.4	* § ||	0.000
	PSD	1.5 ± 0.6	3.0 ± 1.0	2.2 ± 1.0	2.3 ± 0.9	* †	0.000
A-4/2	MS	3.0 ± 1.7	1.3 ± 0.7	2.6 ± 1.4	2.5 ± 1.1	* § ||	0.000
	MD	−0.2 ± 1.8	−1.1 ± 1.6	−0.1 ± 1.8	−0.3 ± 3.0	* § ||	0.003
	PSD	2.3 ± 0.8	3.9 ± 1.2	3.1 ± 1.3	3.6 ± 1.7	* † ‡ §	0.000
A-4/12	MS	2.0 ± 1.2	0.9 ± 0.8	1.8 ± 1.2	1.7 ± 0.5	* §	0.000
	MD	0.2 ± 1.8	−0.4 ± 1.5	0.8 ± 2.3	−0.0 ± 2.3	None	0.050
	PSD	2.4 ± 1.1	3.4 ± 1.4	3.0 ± 0.9	3.8 ± 1.6	* † ‡	0.000
BY-0.5/2	MS	5.2 ± 1.6	2.6 ± 1.6	5.1 ± 1.9	5.0 ± 1.3	* § ||	0.000
	MD	−0.3 ± 1.3	−1.6 ± 1.7	0.3 ± 1.3	−0.0 ± 1.6	* § ||	0.000
	PSD	1.3 ± 0.3	2.3 ± 0.6	1.8 ± 0.5	2.1 ± 0.8	* † ‡	0.000
BY-0.5/12	MS	1.4 ± 1.1	0.8 ± 0.9	1.4 ± 1.0	1.4 ± 1.4	* §	0.017
	MD	0.1 ± 1.2	1.6 ± 3.3	1.3 ± 1.7	1.5 ± 1.9	† ‡	0.000
	PSD	1.6 ± 0.8	1.8 ± 2.0	1.4 ± 1.2	1.0 ± 1.1	None	0.066
RG-0.5/2	MS	3.2 ± 0.9	1.8 ± 1.1	2.8 ± 1.3	2.8 ± 1.2	* §	0.000
	MD	0.2 ± 0.9	−0.9 ± 1.2	0.1 ± 1.4	−0.4 ± 1.1	*	0.004
	PSD	1.6 ± 0.7	2.3 ± 0.4	1.8 ± 0.5	1.9 ± 0.5	* † ‡	0.000
RG-0.5/12	MS	1.3 ± 0.6	0.7 ± 0.7	1.3 ± 0.7	1.4 ± 1.3	* §	0.000
	MD	0.6 ± 0.8	0.1 ± 0.9	0.7 ± 1.0	0.6 ± 1.4	* §	0.002
	PSD	1.4 ± 0.4	2.0 ± 0.4	1.6 ± 0.5	1.9 ± 0.5	* ‡ §	0.000

The data are expressed in dB as the mean ± standard deviation.
* N versus G.
† N versus OHT-S.
‡ N versus RNFL-S.
§ G versus OHT-S.
|| G versus RNFL-S.

ROC curves, were used to compare the diagnostic capabilities of the different stimuli (see Table 4). Note that sensitivities for 85% specificity obtained this way, which are the same as those derived in step 5, slightly differ from the values derived by interpolating the CDFs (step 4) due to finite sample size.

Ethics

The use of the ATD device in this study was approved by the Research Commission of Institut Català de Retina and the Ethics Committee of the Hospital Universitari Sagrat Cor. The study complied with the tenets of the Declaration of Helsinki.

RESULTS

ATD Global Indices

The MS values (Table 2) were significantly lower in G than in N subjects for all eight stimuli, and also lower than in glaucoma suspects for most stimuli. Differences in MS between N, OHT-S, and RNFL-S were not significant (Table 2). For this reason, in the rest of the analysis we focus only on global indices MD and PSD.

MD was significantly lower in G eyes than in N subjects for all types of stimuli except A-4/12 and BY-0.5/12 (Table 2). The MD showed similar values in N, OHT-S, and RNFL-S. Nevertheless, BY-0.5/12 did show significant, and paradoxical, differences between N and RNFL-S and between N and OHT-S.

The PSD identified differences among all groups (Table 2) with most stimuli. The PSDs of N eyes were significantly lower than those of G eyes for all stimuli, except again for BY-0.5/12, and lower than in all pathology groups for A-0.5/12, A-4/2, A-4/12, BY-0.5/2, and RG-0.5/2. In addition, A-0.5/24 stimuli showed significant differences between N and OHT-S and between N and G. The results with employment of certain stimuli revealed differences between glaucoma patients and glaucoma suspects. Stimuli A-0.5/12, A-4/2, and RG-0.5/12 presented significantly greater PSD in G than in OHT-S, but only PSD for A-0.5/12 in G was also significantly greater than in RNFL-S and OHT-S.

Cumulative Distribution Functions

The CDFs computed for the different stimuli, including all participants from all groups, were much closer together for MD (Fig. 3a) than for PSD (Fig. 4a), suggesting that the latter could be a better index to characterize the functional profiles of the different ATD tests. Curves of a single stimulus type for the four diagnostic groups showed the functional profile of the various clinical situations. The achromatic test A-0.5/12 was the best-performing test to identify glaucoma cases with MD (Fig. 3b), and the glaucoma cumulative curve is clearly separated from those of N, OHT-S, and RNFL-S, which are grouped together. In contrast, the CDFs for BY-0.5/2 PSD (Fig. 4b) showed four distinct profiles for each group, indicating that this test could differentiate among them.

Classification with Global Indices

MD and PSD were able to distinguish between groups but behaved differently. With MD, the tests that identified more

TABLE 3. Case Classification Using ATD Mean Defect and Pattern Standard Deviation

Stimuli	Par.	G %	G Hits/Total	OHT-S %	OHT-S Hits/Total	RNFL-S %	RNFL-S Hits/Total	G+RNFL-S %	G+RNFL-S Hits/Total	Groups with Significant Differences (*P* Value)
A-0.5/12	MD	76.9	28/37	8.0	1/22	8.0	1/13	58.7	29/50	(*P* = 0.000),* (*P* = 0.000),§ (*P* = 0.000)‖
	PSD	58.1	22/37	17.7	4/22	3.6	1/13	45.0	23/50	(*P* = 0.000),* (*P* = 0.002),§ (*P* = 0.001)‖
A-0.5/24	MD	54.7	19/35	8.7	1/19	0.0	0/13	39.9	19/48	(*P* = 0.00),* (*P* = 0.000),§ (*P* = 0.001)‖
	PSD	77.1	27/35	43.2	9/19	38.2	5/13	66.6	32/48	(*P* = 0.0000),* (*P* = 0.002),† (*P* = 0.048),‡ (*P* = 0.027),§ (*P* = 0.012)‖
A-4/2	MD	23.7	8/34	11.0	2/23	0.0	0/12	17.5	8/46	None (*P* = 0.183)
	PSD	74.2	26/34	40.5	10/23	38.9	5/12	65.7	31/46	(*P* = 0.000),* (*P* = 0.005),† (*P* = 0.036),‡, (*P* = 0.011),§ (*P* = 0.027)‖
A-4/12	MD	22.0	8/37	13.2	2/20	16.2	1/10	19.4	9/47	None (*P* = 0.623)
	PSD	47.2	18/37	28.4	6/20	47.0	5/10	47.8	23/47	(*P* = 0.000),* (*P* = 0.013)‡
BY-0.5/2	MD	47.0	13/28	10.3	1/11	17.9	1/11	36.4	14/39	(*P* = 0.001),* (*P* = 0.029),§ (*P* = 0.029)‖
	PSD	81.6	23/28	51.8	6/11	72.2	8/11	79.2	31/39	(*P* = 0.000),* (*P* = 0.005),† (*P* = 0.000)‡
BY-0.5/12	MD	17.1	6/37	7.3	1/23	9.3	1/13	14.4	7/50	None (*P* = 0.509)
	PSD	24.2	9/37	15.6	4/23	3.6	1/13	20.0	10/50	None (*P* = 0.490)
RG-0.5/2	MD	46.0	12/28	31.1	3/12	43.0	5/12	44.5	17/40	(*P* = 0.003),* (*P* = 0.024)‡
	PSD	86.7	25/28	44.5	6/12	41.2	5/12	74.7	30/40	(*P* = 0.000),* (*P* = 0.008),† (*P* = 0.039),‡ (*P* = 0.006),§ (*P* = 0.001)‖
RG-0.5/12	MD	46.3	18/39	18.5	4/23	24.5	3/13	40.5	21/52	(*P* = 0.000),* (*P* = 0.022)§
	PSD	52.4	21/39	16.7	4/23	48.4	7/13	52.7	28/52	(*P* = 0.000),* (*P* = 0.003)‡

The percentages in this table were obtained by interpolation from the Kaplan-Meier CDFs, that slightly differ from hits/total ratios that are shown in the text. The number of hits and the total number of subjects were computed directly from our sample and used in a χ^2 test of significant differences between groups. Par., parameter.

* N versus G.
† N versus OHT-S.
‡ N versus RNFL-S.
§ G versus OHT-S.
‖ G versus RNFL-S.

glaucoma cases as ONL were those that favor the magnocellular pathway, A-0.5/12 and A-0.5/24, which classified as ONL 76.9% (number of cases [*n*] = 28) and 54.7% (*n* = 19), respectively (Table 3; remember that the percentages in this table were calculated by interpolation from the Kaplan-Meier CDFs). The ability of MD to identify damage in suspects was low for most stimuli. Only RG-0.5/2 and RG-0.5/12 classified at least 15% of OHT-S (25.0% and 17.4%, respectively) or RNFL-S

(41.7% and 23.1%, respectively) as ONL. With the PSD (Table 3), the highest ability to identify functional damage in glaucoma cases was demonstrated by the two chromatic stimuli with low spatial frequency, BY-0.5/2 and RG-0.5/2, which were ONL in 82.1% (*n* = 23) and 89.3% (*n* = 25) of G eyes (Table 3).

Both tests were also capable of identifying damage in a significant proportion of OHT-S (50.0% and 17.4%, respective-

TABLE 4. Diagnostic Accuracy of ATD Global Indices for the Classification of Normal and Glaucoma Cases

	Stimulus Type	Highest Value of (sen+spe)/2 G	OHT-S	RNFL-S	Specificity at Highest Value of (sen+spe)/2 G	OHT-S	RNFL-S	Sensitivity at Highest Value of (sen+spe)/2 G	OHT-S	RNFL-S	Sensitivity at 85% Specificity G	OHT-S	RNFL-S
Mean defect, dB	A-0.5/12	82.2	50.6	50.6	88.6	96.6	1.1	75.7	4.5	100.0	75.7	4.5	7.7
	A-0.5/24	75.1	52.0	50.0	73.1	98.7	100.0	77.1	5.3	0	54.3	5.3	0
	A-4/2	69.4	55.1	50.2	50.6	66.7	42.0	88.2	43.5	58.3	23.5	13.0	0
	A-4/12	64.9	54.5	54.1	54.1	54.1	8.1	75.7	55.0	100.0	29.7	10.0	10.0
	BY-0.5/2	68.3	50.4	51.9	54.4	28.1	94.7	82.1	72.7	9.1	46.4	9.1	9.1
	BY-0.5/12	53.2	52.2	50.5	90.2	100.0	1.1	16.2	4.3	100.0	16.2	4.3	7.7
	RG-0.5/2	70.3	60.8	64.8	65.5	96.6	87.9	75.0	25.0	41.7	42.9	25.0	41.7
	RG-0.5/12	68.9	54.8	59.7	83.9	96.6	65.5	53.8	13.0	53.8	51.4	17.4	23.1
Pattern standard deviation, dB	A-0.5/12	82.0	69.3	67.7	69.3	52.3	43.2	94.6	86.4	92.3	59.5	18.2	7.7
	A-0.5/24	**82.2**	**70.2**	**66.7**	87.2	66.7	48.7	77.1	73.7	84.6	**77.1**	**47.4**	**38.5**
	A-4/2	83.2	66.9	71.0	75.3	55.6	75.3	91.2	78.3	66.7	76.5	43.5	41.7
	A-4/12	79.7	71.3	72.4	67.6	67.6	64.9	91.9	75.0	80.0	48.6	30.0	50.0
	BY-0.5/2	**86.7**	**76.2**	**82.9**	91.2	61.4	93.0	82.1	90.9	72.7	**82.1**	**54.5**	**72.7**
	BY-0.5/12	58.4	54.9	50.0	92.4	92.4	92.4	24.3	17.4	7.7	24.3	17.4	7.7
	RG-0.5/2	**87.7**	**68.1**	**69.7**	86.2	86.2	81.0	89.3	50.0	58.3	**89.3**	**50.0**	**41.7**
	RG-0.5/12	75.2	59.4	70.4	73.6	66.7	79.3	76.9	52.2	61.5	53.9	17.4	53.8

Boldface is used to highlight the best results obtained with the parameter highest values of (sen+spe)/2. Sen, sensitivity; Spe, specificity.
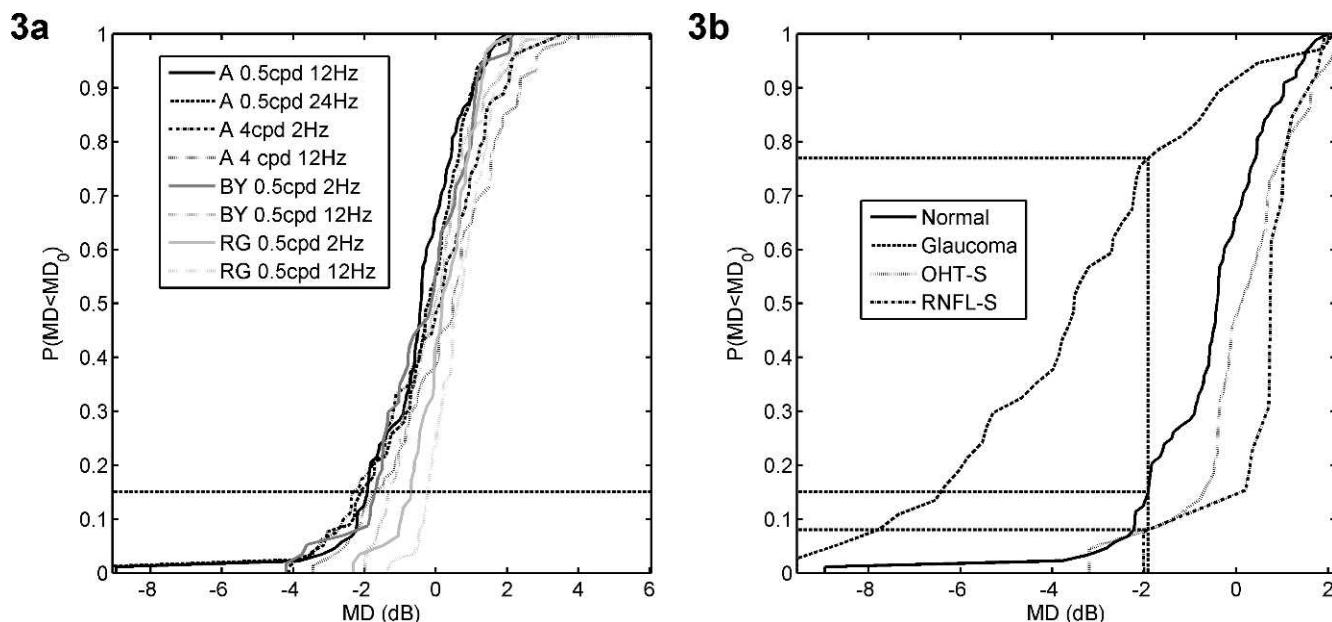
FIGURE 3. Kaplan-Meier cumulative distribution functions of mean defect of ATD by stimulus and by group. (**a**) Distribution of cases from the normal group along the range of MD values for the eight different types of stimuli. (**b**) Cumulative distribution functions of the four groups with the best-performing stimulus, A-0.5/12.

ly) and RNFL-S (41.7% and 53.8%, respectively) eyes. The A-0.5/24 test, similar to FDT stimuli, and the parvocellular A-4/2 test indicated that 77.1% and 76.5% of glaucomatous eyes, respectively, were ONL.

By combining the glaucoma and RNFL-S groups, we evaluated ATD performance if glaucomatous damage had been defined by structural criteria only. In this situation, the PSD of ATD was ONL in 46.0% to 79.5% of cases, excluding the paradoxical results for BY-0.5/12. The most sensitive tests were the achromatic A-0.5/24 (66.7%, $n = 32$) and A-4/2 (67.4%, $n = 31$), together with the blue-yellow BY-0.5/2 (79.5%, $n = 31$) and the red-green RG-0.5/2 (75%, $n = 30$).

Table 4 shows different parameters characterizing the ROC curves shown in Figure 5. The parameters chosen were the point of best equilibrium between sensitivity and specificity (denoted by "Highest Value of (sen+spe)/2" in the table), the specificity and sensitivity at this point, and the values of the sensitivity at 85% specificity. PSD was, in general, a better classifier with these two parameters, and this would also show if the area under the ROC curve was used as the criterion for comparison (see Fig. 5, numerical data not shown). The best-
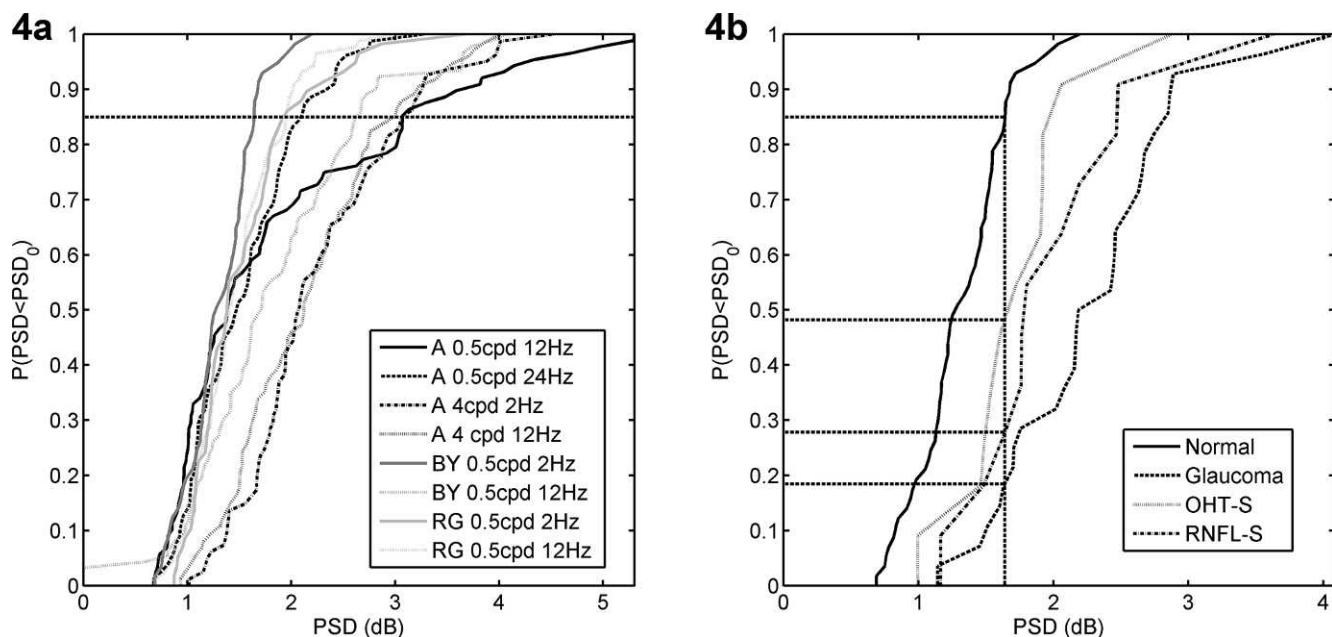
FIGURE 4. Kaplan-Meier cumulative distribution functions of pattern standard deviation of ATD by stimulus and by group. (**a**) Distribution of cases from the normal group along the range of PSD values for the eight different types of stimuli. (**b**) Cumulative distribution functions of the four groups with the best-performing stimulus, BY-0.5/2.
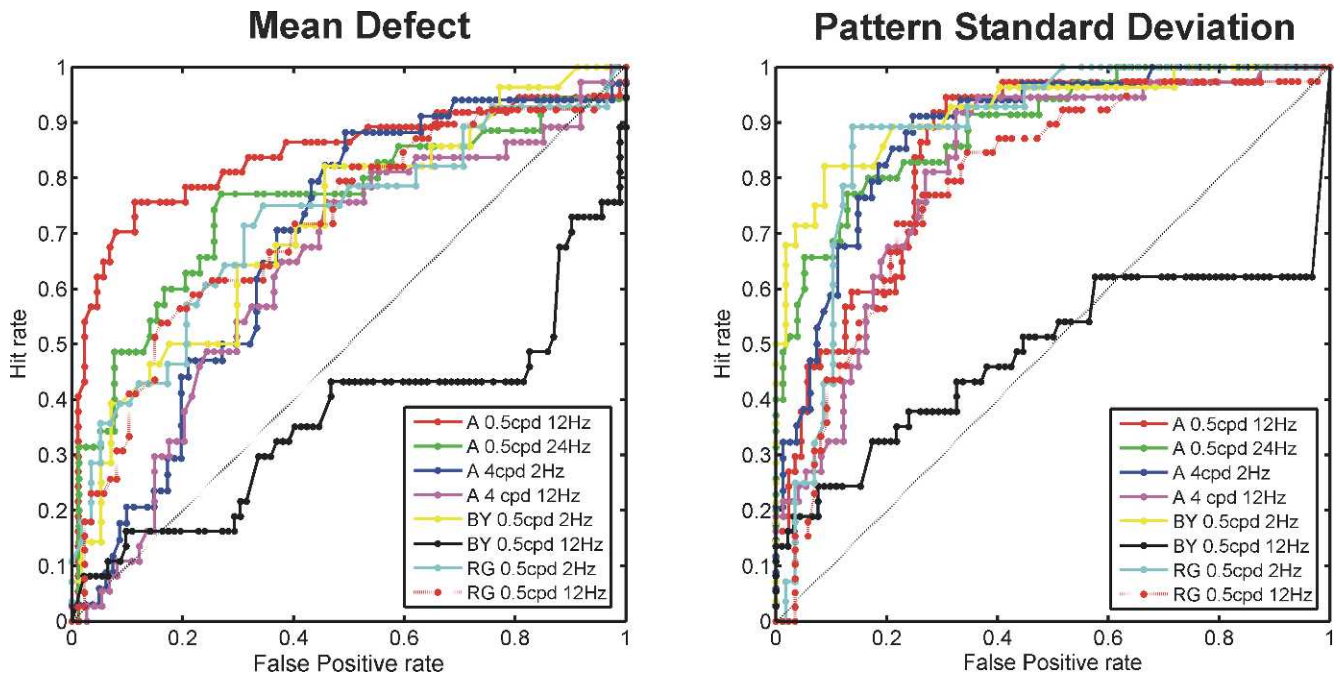
Mean Defect

Pattern Standard Deviation

FIGURE 5. Receiver operating characteristic curves for all stimuli types with ADT indices MD and PSD for the classification of glaucoma and normal cases. PSD was a better classifier with larger areas under the curves. Best-performing ATD stimuli are RG-0.5/2 (*light blue*), BY-0.5/2 (*yellow*), and A-0.2-24 (*green*).

performing ATD stimuli were RG-0.5/2 (light blue), BY-0.5/2 (yellow), and A-0.2-24 (green).

DISCUSSION

Glaucomatous functional damage is complex and alters multiple aspects of visual function, from contrast sensitivity to motion detection. Recent studies have shown that the sensitivity of FDT, SWAP, or HPRP is similar to that of SAP.[27] With ATD, different aspects of visual function may be assessed with a common psychophysical task and with stimuli of equal size and type that can be modulated to favor a certain visual pathway. The two achromatic tests (A-0.5/12 and A-0.5/24) belong to the low spatial–high temporal region where spatial-frequency doubling occurs and possibly favors the magnocellular pathway, although recent evidence indicates that the SAP size III stimulus induced a greater contrast gain between M and P cells than frequency-doubling stimulus in in vivo macaque ganglion cell preparations.[11] The other two ATD achromatic tests (A-4/2 and A-4/12) favor the parvocellular pathway; the red-green stimuli favor the parvocellular pathway; and the blue-yellow stimuli favor the koniocellular pathway. Note, however, that we are using the term *favor* and not the term *isolate* when referring to any given mechanism.

The analysis of the ROC curves showed that ATD was not the desired ideal test to identify glaucoma but indicated that ATD allows identification of the disease with sensitivity and specificity ranging from 80% to 90% for the best tests and cut points. ATD MS was not a good index for classification purposes, as is the case in many other perimeters. ATD MD, obtained by comparing each problem observer with only those normal observers of the same age group, identified significant differences between normal and glaucoma eyes, but was unable to detect disparities in the functional pattern between normal and suspect (with the single exception of A-0.5/12) or between suspects and glaucoma cases. ATD PSD was generally more sensitive than MD to identify cases outside normal limits,

most probably due to glaucomatous damage, as is clearly shown by the ROC curves (Fig. 5); this was not surprising considering that glaucoma cases had early to moderate disease. ATD PSD was also promisingly useful for identifying disparities between normal eyes and suspect eyes or between glaucoma cases and glaucoma suspects with normal SAP. Sample et al.[27] reported similar superiority in diagnostic ability of PSD over MD for FDT, SWAP, and SAP when discriminating between normal and glaucoma eyes, and for FDT, SWAP, HPRP, and SAP for identifying eyes with glaucomatous optic disc changes. ATD PSD demonstrated sensitivity to identify early functional damage. It yielded ONL results in up to 54% of ocular hypertensive patients and in up to 72% of eyes with structural damage and normal SAP.

Different ATD stimuli offer different results in normal subjects and glaucoma and suspect patients. Globally, the two chromatic stimuli with low spatial frequency (BY-0.5/2 and RG-0.5/2) were the most sensitive, identifying functional results ONL in all study groups. The first, a blue-yellow stimulus that favors the koniocellular pathway, appeared to be a bit more sensitive to detect early damage in eyes with normal SAP. It found damage in 51.8% of OHT-S and 72.2% of RNFL-S, figures that are slightly higher than those obtained by SWAP. SWAP identified functional damage in 33.3% in RNFL-S by OCT[19] and the 10% to 30% of OHT-S eyes.[37] The second chromatic stimulus with low spatial frequency (RG-0.5/2), a red-green stimulus that favors the parvocellular pathway, had a bit more sensitivity to identify glaucoma (89.3% ONL) and was also able to identify functional deficits in 44.5% of OHT-S and 41.2% of RNFL-S. HPRP, the parvocellular test best studied in the literature, has shown capability to detect damage in 12%[24] of glaucoma suspects and 15% to 24% of OHT-S eyes.[27] Additionally, ATD test A-0.5/24, which has very similar characteristics to FDT, was ONL in 77.1% of G, 43.2% of OHT-S; and 38.2% of RNFL-S. FDT has been demonstrated to be ONL[10,19,27,38] in 67.7% to 91% of glaucoma eyes, in 10% to 45.3% of OHT-S, and in 28.5% to 33% of RNFL-S—figures that are similar to those for the A-0.5/24 ATD test but slightly lower

than those for the best ATD stimuli. Nevertheless, the criteria used to select the sample and to qualify a certain test result as ONL were different in each study, and these differences make direct comparison a difficult and risky task.

The cut points selected in this study were based on the CDFs and aimed at the 85% limits of normality; and this definition could, as with any other, directly influence and apparently increase or decrease the rate of cases ONL. Additionally, there is no consensus and probably not sufficient solid data to define the visual function of glaucoma suspects apart from the fact that they have, by definition, normal SAP. For this reason it is not possible to affirm with certainty whether ATD abnormal results are truly positive cases with early glaucomatous functional damage or false-positive results.

The results suggested that ATD could help to identify differences in the degree or pattern of functional damage of OHT-S and RNFL-S using certain achromatic stimuli (A-0.5/12 or A-4/2) or a red-green test (RG-0.5/12). Finally, the blue-yellow stimulus BY-0.5/12 deserves special mention in that it behaved paradoxically, showing higher MD values in ocular hypertensive patients and glaucoma suspects than in normal subjects and yielding lower PSD values in ocular hypertensive patients and glaucoma suspects than in normal or glaucomatous eyes. This could have been due to unexpected behavior of damaged ganglion cells, or more likely, an artifact or a consequence of the methods. Independently of the reason, ATD BY-0.5/12 should not be used until more information is available.

This study has some limitations. First, isolating a visual mechanism is not a simple task. We used stimuli generated along the cardinal directions of the opponent modulation space; but for any real observer, the direction isolating the red-green mechanism depends on the relative L and M contribution to the achromatic mechanism. Since this relative contribution was not individually determined, it could introduce an achromatic artifact, and therefore some detections could be mediated by an undesired mechanism.[39] The main difficulty arises from the fact that these relative cone contributions are estimated through determination of the isoluminant condition for the observer, and this condition depends on the spatial frequency and the spatial location of the stimulus.[40] To make a single determination of the isoluminant condition, for instance for just one spatial frequency at the fovea, would not eliminate the problem; and to repeat the procedure for each point in the spatiotemporal domain used in the experiment would not be feasible in clinical practice. Conversely, working with the cardinal directions of the standard observer could result in wider probability density functions, and the potential sensitivity for pathology detection using this kind of stimulus could be decreased.

A second problem is related to the difficulties involved in assessment of the achromatic mechanism. Our subjects responded whenever they perceived a change in the background, regardless of the appearance of the stimulus. Some reports indicate that there is no difference between detection and pattern recognition thresholds, and that detection occurs with recognition of the spatial pattern and therefore with perception of the frequency-doubling effect.[41,42] We cannot be sure of what our observers perceived when seeing a low-spatial-frequency and high-temporal-frequency ATD stimulus at threshold, and therefore it is not possible to discard some contribution of the parvocellular pathway.[43]

Another possible source of bias is the fact that the same set of subjects was used as normative database to derive the MD and PSD values and as the sample of normals with whom we are comparing the pathological subjects (control group). However, by repeating the analysis shown in this paper with disjoint sets of control and normative subjects, randomly extracted from the entire database, we have found that with regard to general trends, the conclusions we present here still hold.

Finally, it is probably ideal to assess functional tests defining the sample groups based only on structural damage criteria. Nevertheless, for this first study we chose frequently used definitions to make our data more comparable to previous published data. Additionally, this study estimated the behavior of ATD considering only structural criteria to define glaucomatous damage (Table 3). In this situation, PSD of ATD was able to identify functional damage in 44.5% to 79.5% of cases. Boden et al.[44] assessed SAP and FDT on eyes with glaucomatous optic neuropathy and found functional damage in 43.2% of cases with FDT and in 40.3% with SAP.

In summary, the ATD functional modulator was capable of assessing different aspects of optic nerve function using eight distinct stimuli. PSD was the most sensitive index to identify functional damage in glaucoma. Of the eight ATD stimuli assessed, the most sensitive to detect glaucomatous damage were the low-temporal-frequency chromatic tests (BY-0.5/2 and RG-0.5/2). Some of the ATD functional tests could be more sensitive than presently used perimeters, but further clinical studies are needed to confirm this. Moreover, certain global indices and certain stimuli seemed to be more sensitive to initial functional changes in OHT-S and RNFL-S, suggesting that certain tests could be more adequate than others depending on the subject to be examined. Further evaluation is needed to establish which particular ATD test type or types should be recommended to detect and follow glaucoma over time.

References

1. European Glaucoma Society. *Terminology and Guidelines for Glaucoma*. 3rd ed. Savona, Italy: Dogma; 2008.

2. Quigley HA, Addicks EM, Green WR. Optic nerve damage in human glaucoma. III. Quantitative correlation of nerve fiber loss and visual field defect in glaucoma, ischemic neuropathy, papilledema, and toxic neuropathy. *Arch Ophthalmol*. 1982; 100:135–146.

3. Quigley HA, Dunkelberger GR, Green WR. Retinal ganglion cell atrophy correlated with automated perimetry in human eyes with glaucoma. *Am J Ophthalmol*. 1989;107:453–464.

4. Harwerth RS, Carter-Dawson L, Shen F, Smith EL III, Crawford ML. Ganglion cell losses underlying visual field defects from experimental glaucoma. *Invest Ophthalmol Vis Sci*. 1999;40: 2242–2250.

5. Johnson CA, Adams AJ, Twelker JD, Quigg JM. Age-related changes in the central visual field for short-wavelength-sensitive pathways. *J Opt Soc Am A*. 1988;5:2131–2139.

6. Sample PA, Johnson CA, Haegerstrom-Portnoy G, Adams AJ. Optimum parameters for short-wavelength automated perimetry. *J Glaucoma*. 1996;5:375–383.

7. McKendrick AM, Badcock DR, Morgan WH. The detection of both global motion and global form is disrupted in glaucoma. *Invest Ophthalmol Vis Sci*. 2005;46:3693–3701.

8. Sample PA, Bosworth CF, Weinreb RN. Short-wavelength automated perimetry and motion automated perimetry in patients with glaucoma. *Arch Ophthalmol*. 1997;115:1129–1133.

9. Johnson CA, Cioffi GA, Van Buskirk EM. Frequency doubling technology perimetry using a 24-2 stimulus presentation pattern. *Optom Vis Sci*. 1999;76:571–581.

10. Quigley HA. Identification of glaucoma-related visual field abnormality with the screening protocol of frequency doubling technology. *Am J Ophthalmol*. 1998;125:819–829.

11. Swanson WH, Sun H, Lee BB, Cao D. Responses of primate retinal ganglion cells to perimetric stimuli. *Invest Ophthalmol Vis Sci*. 2011;52:764–771.

12. White AJ, Sun H, Swanson WH, Lee BB. An examination of physiological mechanisms underlying the frequency-doubling illusion. *Invest Ophthalmol Vis Sci*. 2002;43:3590–3599.

13. Vidal-Fernandez A, Garcia Feijoo J, Gonzalez-Hernandez M, Gonzalez De La Rosa M, Garcia Sanchez J. Initial findings with pulsar perimetry in patients with ocular hypertension. *Arch Soc Esp Oftalmol*. 2002;77:321–326.

14. Zeppieri M, Brusini P, Parisi L, Johnson CA, Sampaolesi R, Salvetat ML. Pulsar perimetry in the diagnosis of early glaucoma. *Am J Ophthalmol*. 2009;149:102–112.

15. Zeppieri M, Demirel S, Kent K, Johnson CA. Perceived spatial frequency of sinusoidal gratings. *Optom Vis Sci*. 2008;85:318–329.

16. Chauhan BC, LeBlanc RP, McCormick TA, Rogers JB. Comparison of high-pass resolution perimetry and pattern discrimination perimetry to conventional perimetry in glaucoma. *Can J Ophthalmol*. 1993;28:306–311.

17. Wanger P, Persson HE. Pattern-reversal electroretinograms and high-pass resolution perimetry in suspected or early glaucoma. *Ophthalmology*. 1987;94:1098–1103.

18. Cellini M, Torreggiani A. Frequency doubling perimetry in ocular hypertension and chronic open angle glaucoma. *Acta Ophthalmol Scand Suppl*. 2002;236:24–25.

19. Ferreras A, Polo V, Larrosa JM, et al. Can frequency-doubling technology and short-wavelength automated perimetries detect visual field defects before standard automated perimetry in patients with preperimetric glaucoma? *J Glaucoma*. 2007;16:372–383.

20. Wu LL, Suzuki Y, Kunimatsu S, Araie M, Iwase A, Tomita G. Frequency doubling technology and confocal scanning ophthalmoscopic optic disc analysis in open-angle glaucoma with hemifield defects. *J Glaucoma*. 2001;10:256–260.

21. Soliman MA, de Jong LA, Ismaeil AA, van den Berg TJ, de Smet MD. Standard achromatic perimetry, short wavelength automated perimetry, and frequency doubling technology for detection of glaucoma damage. *Ophthalmology*. 2002;109:444–454.

22. van der Schoot J, Reus N, Colen T, Lemij H. The ability of short-wavelength automated perimetry to predict conversion to glaucoma. *Ophthalmology*. 2010;117:30–34.

23. Meyer JH, Funk J. High-pass resolution perimetry and light-sense perimetry in open-angle glaucoma. *Ger J Ophthalmol*. 1995;4:222–227.

24. Martinez GA, Sample PA, Weinreb RN. Comparison of high-pass resolution perimetry and standard automated perimetry in glaucoma. *Am J Ophthalmol*. 1995;119:195–201.

25. Derrington AM, Krauskopf J, Lennie P. Chromatic mechanisms in lateral geniculate nucleus of macaque. *J Physiol*. 1984;357:241–265.

26. Merigan W, Maunsell J. How parallel are the primate visual pathways? *Annu Rev Neurosci*. 1993;16:369–402.

27. Sample PA, Medeiros FA, Racette L, et al. Identifying glaucomatous vision loss with visual-function-specific perimetry in the diagnostic innovations in glaucoma study. *Invest Ophthalmol Vis Sci*. 2006;47:3381–3389.

28. Harwerth RS, Smith EL III, DeSantis L. Mechanisms mediating visual detection in static perimetry. *Invest Ophthalmol Vis Sci*. 1993;34:3011–3023.

29. King-Smith PE, Carden D. Luminance and opponent-color contributions to visual detection and adaptation and to temporal and spatial integration. *J Opt Soc Am*. 1976;66:709–717.

30. Kranda K, King-Smith PE. Detection of coloured stimuli by independent linear systems. *Vision Res*. 1979;19:733–745.

31. Johnson CA, Marshall D Jr. Aging effects for opponent mechanisms in the central visual field. *Optom Vis Sci*. 1995;72:75–82.

32. Lynch S, Johnson C, Demirel S. Is early damage in glaucoma selective for a particular cell type or pathway? In: Wall M, Heijl A, eds. *Perimetry Update 1996/1997*. Amsterdam: Kugler Publications; 1997:253–261.

33. Brainard D. Cone contrast and opponent modulation color spaces. In: Kaiser PK, Boynton RM. *Human Color Vision*. Washington, DC: Optical Society of America; 1996:563–579.

34. Krauskopf J, Williams DR, Heeley DW. Cardinal directions of color space. *Vision Res*. 1982;22:1123–1131.

35. Smith VC, Pokorny J. Spectral sensitivity of the foveal cone photopigments between 400 and 500 nm. *Vision Res*. 1975;15:161–171.

36. Kaplan EL, Meier P. Nonparametric estimation from incomplete observations. *J Am Stat Assoc*. 1958;53:457–481.

37. Johnson CA, Brandt JD, Khong AM, Adams AJ. Short-wavelength automated perimetry in low-, medium-, and high-risk ocular hypertensive eyes. Initial baseline results. *Arch Ophthalmol*. 1995;113:70–76.

38. Brusini P, Busatto P. Frequency doubling perimetry in glaucoma early diagnosis. *Acta Ophthalmol Scand Suppl*. 1998;227:23–24.

39. Stromeyer CFI, Chaparro A, Tolias AS, Kronauer RE. Colour adaptation modifies the long-wave and middle-wave cone weights and temporal phases in human luminance (but not red-green) mechanisms. *J Physiol*. 1997;499:227–254.

40. Bilodeau L, Faubert J. Isoluminance and chromatic motion perception throughout the visual field. *Vision Res*. 1997;37:2073–2081.

41. Hogg R, Anderson A. Appearance of the frequency-doubling stimulus at threshold. *Invest Ophthalmol Vis Sci*. 2009;50:1477–1482.

42. Vallam K, Metha A. Spatial structure of the frequency doubling illusion. *Vision Res*. 2007;47:1732–1744.

43. White A, Sun H, Swanson W, Lee B. An examination of physiological mechanisms underlying the frequency-doubling illusion. *Invest Ophthalmol Vis Sci*. 2002;43:3590–3599.

44. Boden C, Pascual J, Medeiros FA, Aihara M, Weinreb RN, Sample PA. Relationship of SITA and full-threshold standard perimetry to frequency-doubling technology perimetry in glaucoma. *Invest Ophthalmol Vis Sci*. 2005;46:2433–2439.